Validation of a new "3D calorimetry" of hot nuclei with the HIPSE event generator

E. Vient,[1,*] L. Manduci,[1,2] E. Legouée,[1] L. Augey,[1] E. Bonnet,[3] B. Borderie,[4] R. Bougault,[1] A. Chbihi,[5] D. Dell'Aquila,[4,6] Q. Fable,[5] L. Francalanza,[6] J. D. Frankland,[5] E. Galichet,[4,7] D. Gruyer,[1,8] D. Guinet,[9] M. Henri,[1] M. La Commara,[6] G. Lehaut,[1] N. Le Neindre,[1] I. Lombardo,[6,10] O. Lopez,[1] P. Marini,[11] M. Pârlog,[1,12] M. F. Rivet,[4,†] E. Rosato,[6,†] R. Roy,[13] P. St-Onge,[5,13] G. Spadaccini,[6] G. Verde,[4,10] and M. Vigilante[6]

[1]*Normandie Univ, ENSICAEN, UNICAEN, CNRS/IN2P3, LPC Caen, F-14000 Caen, France*
[2]*École des Applications Militaires de l'Énergie Atomique, B.P. 19, F-50115 Cherbourg, France*
[3]*SUBATECH UMR 6457, IMT Atlantique, Université de Nantes, CNRS-IN2P3, 44300 Nantes, France*
[4]*Institut de Physique Nucléaire, CNRS/IN2P3, Univ. Paris-Sud, Université Paris-Saclay, F-91406 Orsay cedex, France*
[5]*Grand Accélérateur National d'Ions Lourds (GANIL), CEA/DRF-CNRS/IN2P3, Bvd. Henri Becquerel, 14076 Caen, France*
[6]*Dipartimento di Fisica 'E. Pancini' and Sezione INFN, Universitá di Napoli 'Federico II', I-80126 Naples, Italy*
[7]*Conservatoire National des Arts et Métiers, F-75141 Paris Cedex 03, France*
[8]*Sezione INFN di Firenze, Via G. Sansone 1, I-50019 Sesto Fiorentino, Italy*
[9]*IPNL/IN2P3 et Université de Lyon/Université Claude Bernard Lyon1, 43 Bd du 11 novembre 1918 F69622 Villeurbanne Cedex, France*
[10]*INFN — Sezione Catania, via Santa Sofia 64, 95123 Catania, Italy*
[11]*CEA, DAM, DIF, F-91297 Arpajon, France*
[12]*Hulubei National Institute for R & D in Physics and Nuclear Engineering (IFIN-HH), P.O. BOX MG-6, RO-76900 Bucharest-Màgurele, Romania*
[13]*Laboratoire de Physique Nucléaire, Université Laval, Québec G1K 7P4, Canada*

(Received 27 April 2018; published 16 October 2018)

In nuclear thermodynamics, the determination of the excitation energy of hot nuclei is a fundamental experimental problem. Instrumental physicists have been trying to solve this problem for several years by building the most exhaustive 4π detector arrays and perfecting their calorimetry techniques. In a recent paper, a proposal for a new calorimetry, called "3D calorimetry", was made. It tries to optimize the separation between the particles and fragments emitted by the quasiprojectile and the other possible contributions. This can be achieved by determining the experimental probability for a given nucleus of a nuclear reaction to be emitted by the quasiprojectile. It has been developed for the INDRA data. In the present work, we wanted to dissect and validate this new method of characterization of a hot quasiprojectile. So we tried to understand and control it completely to determine these limits. Using the Heavy Ion Phase Space Exploration (HIPSE) event generator and a software simulating the functioning of INDRA, we were able to achieve this goal and provide a quantitative estimation of the quality of the quasiprojectile characterization.

DOI: 10.1103/PhysRevC.98.044612

I. INTRODUCTION

Heavy-ion collisions in the Fermi energy domain allow the formation of very hot nuclei. We want to study the evolution of these hot nuclei, as the deposited energy increases. We should be able to observe a phase transition of these drops of nuclear matter. But we must keep in mind that the collision processes in this energy range are very complex. In this energy region of 10–100 MeV/nucleon, there is a competition between the effects of the nucleus mean field and the nucleon-nucleon interaction [1,2]. This leads to an evolution of reaction mechanisms [3], which gradually develop from complete (incomplete) fusion or deeply inelastic collisions with a statistical emission towards binary collisions [4–7] accompanied by particle emissions at different equilibration degrees, neck emission [8–12], and preequilibrium [13,14]. It is in this context that the nuclear physicists by means of calorimetry [15] must try to isolate the hot nuclei formed during these processes and to characterize them in the best possible way. "3D calorimetry" is presented in detail in two Refs. [16,17]. The basic idea is that, in a restricted area of the velocity space in the quasiprojectile (QP) frame, we can completely define the spatioenergetic characteristics of the evaporated nuclei by the QP. By comparison with the other areas of the velocity space, the probability for a nucleus produced in the collision to be evaporated by the QP can be determined. Then, event by event, these probabilities are used to reconstruct the QP, i.e., to determine its mass, charge, velocity in the center-of-mass (c.m.) frame and excitation energy. This calorimetry was applied to the data of Xe + Sn reactions acquired with the INDRA detector array [18] at different incident energies. The presented work is devoted to the study and validation of this new experimental calorimetry using the Heavy Ion Phase Space Exploration (HIPSE)

*vient@lpccaen.in2p3.fr; http://caeinfo.in2p3.fr/
†Deceased.

event generator [19]. In addition, a software simulating as realistically as possible all the detection phases by INDRA [20,21] will be used. All the events supplied by HIPSE can be filtered by it. In the first section, the event generator used is qualified by a quantitative comparison with the data obtained by the INDRA collaboration for the system of interest. We want verify that it is realistic and correct enough to be used for calorimetry validation. In the following section we apply the new calorimetry to experimental data and filtered events provided by HIPSE. By means of a systematic comparison between both, we will quantitatively verify the quality of the characterization of the hot QP. In the last section, we conclude this work.

II. QUALIFICATION OF THE HIPSE EVENT GENERATOR

The event generator HIPSE (Heavy Ion Phase Space Exploration) is described in detail in Ref. [19]. HIPSE, compared to commonly used generators, is capable of reproducing most of the processes occurring in heavy-ion collisions at intermediate energies. This is indeed a fundamental contribution. It can manage the preequilibrium phase, the physics of the participating zone, and the phase of deexcitation of the formed hot nuclei, taking into account all the spatiotemporal correlations due to the Coulomb interaction. It thus allows us to go further in the study of the experimental calorimetry.

It is important for our study to check that the event generator is able to correctly take into account the static and dynamic characteristics of collisions studied. This has already been done in part in Ref. [19]. In this paper it is clear that HIPSE, for the system Xe + Sn, is capable of correctly reproducing the charge distributions, the correlations between the charge and the parallel velocity of nuclei produced, the mean kinetic energy according to the charge or to the angle of emission in the center of mass. It allows us to find at 50 MeV/nucleon the distribution of the flow angle for complete events, for which 80% of the initial charge and linear momentum have been detected, as well as the densities of particles per unit of velocity along the beam, for different types of particles, giving a spatial-energetic correlation close to those of the experimental ones. This is fundamental for the analysis we want to perform with the data supplied by this generator. It is also important to note that the requirements used in HIPSE to describe the formation of the clusters at midrapidity or the preequilibrium are also applied in the nIPSE nucleon-nucleus collision model [22]. It is also capable of reproducing very well the physical characteristics of the particles produced during such a collision, as shown by Ref. [22]. To pass all generated events through the INDRA multidetector, the software simulating the entire operation of this apparatus and described in Ref. [20], is always used. The generated events, detected by this virtual detector, will be called filtered events.

A. General characteristics of the collisions

First we will see how the selections of the events used to perform calorimetry of nuclei can be used equally for data and HIPSE. With the help of HIPSE, we also want to estimate the cross sections of detected events and the impact

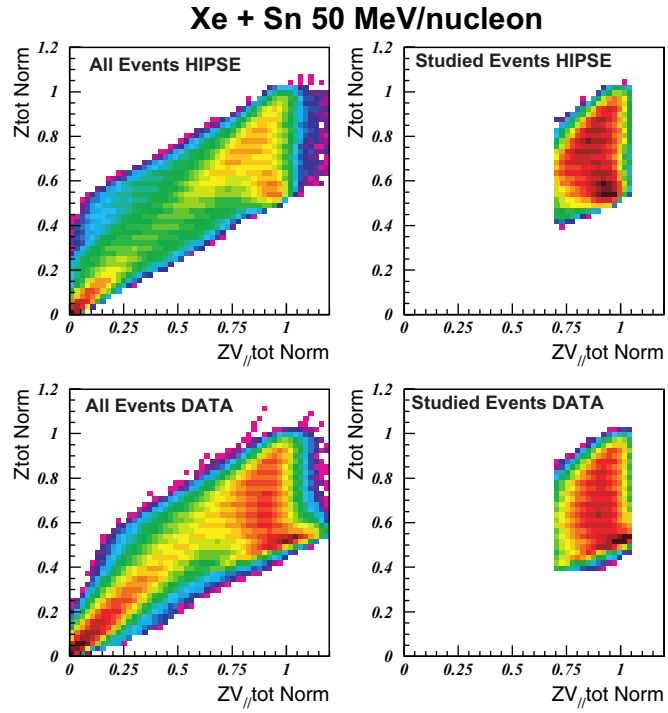

FIG. 1. Two-dimensional graphs giving the total detected charge normalized to the initial total charge as a function of the detected pseudomomentum normalized to the total initial pseudomomentum (the z scale is logarithmic). This is made for the data and for the generator HIPSE, in two cases: with all the events seen by INDRA and with the events said complete at the front of the center of mass.

parameters actually studied. In order to verify the quality of the reaction detection [16,23], Fig. 1 shows, for filtered events, the two-dimensional graphs giving the total detected charge normalized to the initial total charge as a function of the detected pseudomomentum normalized to the total initial pseudomomentum, on the left for all the events actually detected by INDRA and on the right for the studied events, i.e., complete events at the front of the center of mass. For the latter, it is the total pseudomomentum of particles and fragments, located at the front of the c.m., which is normalized to the initial pseudomomentum of the projectile. A perfect detection of an event for all the charged particles produced must be located in this graph at the point of coordinates (1,1). We note a very good qualitative agreement between simulation and data. Figure 2 shows the distributions of the impact parameter given by HIPSE for various event selections in collisions Xe + Sn at 50 MeV/nucleon. We generated 3×10^6 events with impact parameters between 0 and 11 fermis closed for this study. INDRA detected only 85% of these events, i.e., about 70% of the total geometrical cross section. Very peripheral collisions are almost invisible for this incident energy. Our criterion of completeness at the front of the center of mass has further reduced our events, as only about 1/3 of the HIPSE events are selected. It is important to note that this loss is present over the full range of impact parameters as shown again in Figs. 2(a) and 4(a). Various indicative criteria for completeness are presented in Fig. 2(b).

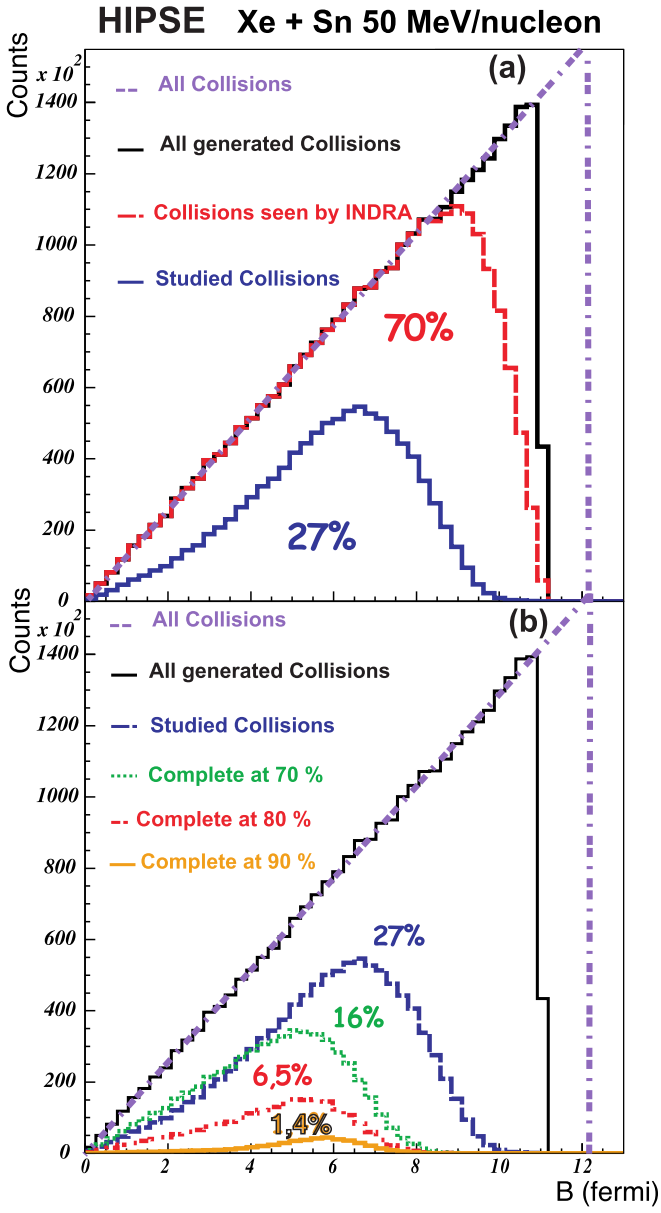

FIG. 2. Distributions of impact parameters generated by HIPSE for different criteria of event completeness. (a) For all the generated events, for events with at least one detected particle and for studied events, i.e., a completeness at the front of the c.m. (b) For all generated events, for studied events, for events with different total completeness.

We immediately see that when we ask for completeness not only in the forward hemisphere of the center of mass but in the whole velocity space, the proportion of the events that satisfy the selection decreases sharply because of the very high detection threshold for emissions from the quasitarget (QT). Finally only 16%, 6.5%, and 1.4% of total geometrical cross sections are retained for completeness requirements of 70%, 80%, and 90% respectively. These criteria eliminate all the events with an impact parameter greater than 8 fm. The 80% completeness criterion has been widely used by the INDRA collaboration. A study, performed by Marie *et al.* [24]

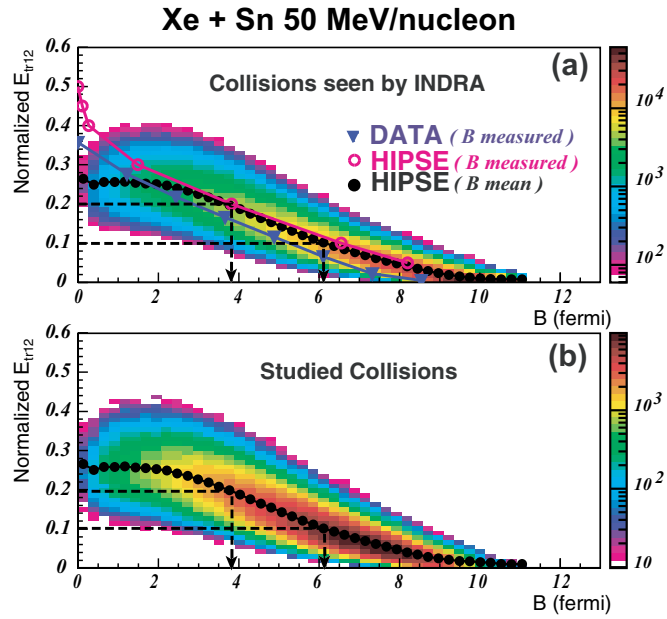

FIG. 3. (a) Two-dimensional graph of the normalized transverse kinetic energy of the particles of $Z \leqslant 2$ as a function of the impact parameter, provided by HIPSE for Xe + Sn at 50 MeV/nucleon, for all the events seen by INDRA. The blue triangles correspond to the average correlation between normalized E_{tr12} and B determined by Marie *et al.* [24]. The pink open circles correspond to the result of the applying experimental technique used in Ref. [24] to the data provided by HIPSE. The full black circles correspond to the average correlation calculated from the two-dimensional graph. (b) For HIPSE only, as in (a), for complete events in the forward hemisphere of the center of mass seen by INDRA. The full black circles correspond to the average correlation calculated from the two-dimensional graph.

on the data Xe + Sn at 50 MeV/nucleon, showed that such a selection represents 12.5% of the events effectively seen by INDRA. If we do an equivalent calculation with HIPSE, we find a close but not identical result of 9.3%.

Experimentally we do not have direct access to the impact parameter. But it can be deduced from an experimental observable strongly correlated with it, see for example Refs. [24–28]. In particular Marie *et al.* [24] used the transverse kinetic energy of the LCPs assuming a maximum impact parameter of 12.2 fm. Figure 3 shows the correlation of this transverse kinetic energy E_{tr12}, normalized to the available energy perpendicular to the direction of the beam in the center of mass, as a function of the impact parameter B, for the system ^{129}Xe + ^{nat}Sn at 50 MeV/nucleon, as supplied by HIPSE. We also drew the mean correlation between these two variables (full black circles). The correlation is shown for all events detected by INDRA in Fig. 3(a) and for those selected by the specific completeness, defined above, at the front of the center of mass in Fig. 3(b). In Fig. 3(a) we can see the mean values of this correlation: the blue triangles represent the result of the calculation applied to the data, performed in Ref. [24] and the pink open circles represent the mean values extracted from HIPSE data with the same method. As can be seen, the agreement between the mean correlation (full

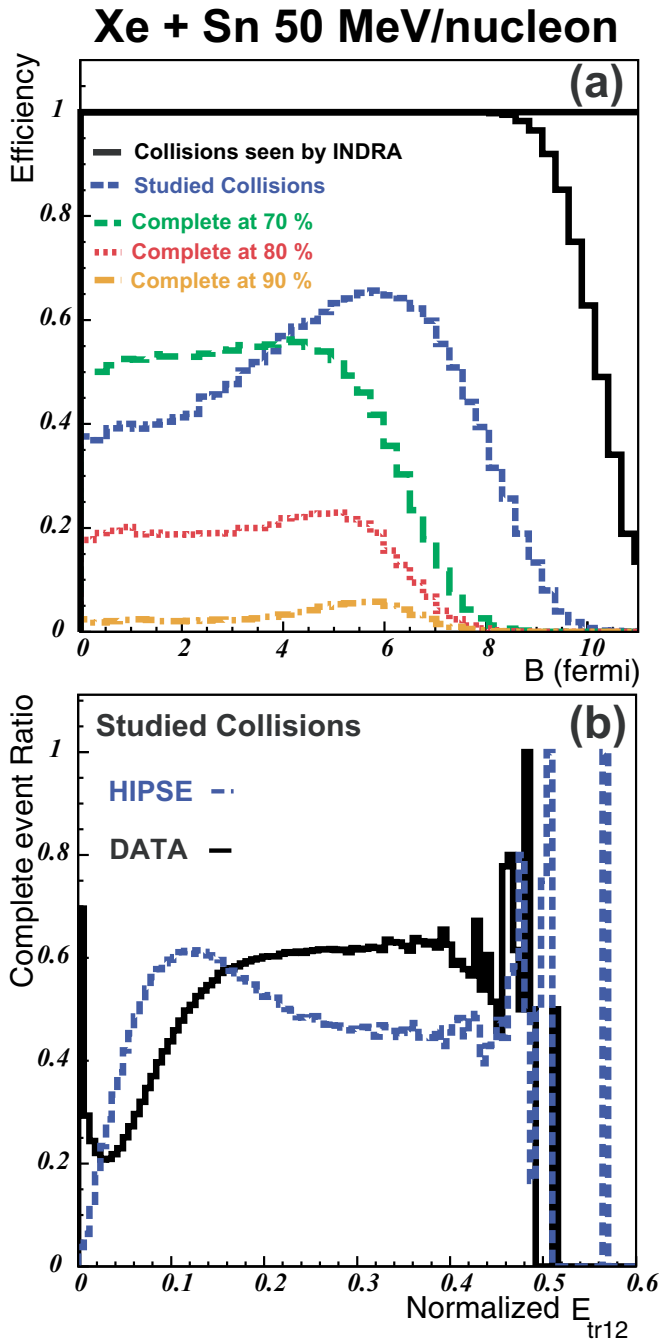

FIG. 4. (a) Average detection efficiency as a function of the impact parameter for different completeness criteria obtained from HIPSE filtering for the system Xe + Sn at 50 MeV/nucleon. (b) Comparison of the average detection efficiency as a function of the normalized E_{tr12} between HIPSE and data.

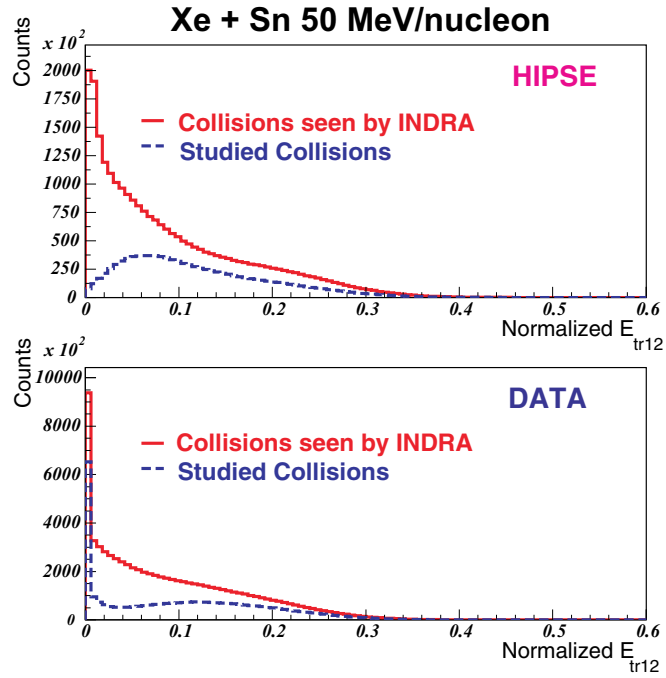

FIG. 5. Comparison of the distributions of normalized E_{tr12} for HIPSE and data for all the detected events and studied events.

black circles) and the calculated average (pink open circles) for HIPSE data is good especially between 2 and 8 fermis. This method is based on the assumption that the efficiency of detecting an event is independent from the impact parameter. Figure 4(a) shows that this hypothesis is not true beyond 8.5 fermis. In Fig. 3 it is important to note that the average correlation for the studied events, in HIPSE, is the same as that for all the events detected by INDRA. Completeness does not interfere with the existing correlation. On the other hand, Fig. 3 shows a systematic discrepancy between data and HIPSE, even if the evolution of the curve is very similar. To understand this difference, we can refer to Fig. 5, where the normalized transverse kinetic energy distributions of LCPs are shown for experimental and simulated events. The number of events studied (blue graph) shows a large difference between data and HIPSE. For data there is a strong contribution for very low values of normalized E_{tr12}, i.e., for very peripheral collisions, which is not the case in the simulation. This seems to indicate, for HIPSE, that the quasiprojectiles, for these very peripheral collisions, are not correctly detected. In addition, we note that HIPSE gives maximum values of transverse kinetic energy slightly higher than the data.

Figure 4 confirms this finding. At the top, the efficiency of event detection, supplied by HIPSE, is presented according to the impact parameter for different completeness criteria. At the bottom in Fig. 4(b), there are the experimental rates of detection of the studied collisions, i.e., complete events in the forward hemisphere of the c.m., as a function of the normalized E_{tr12} for the data and HIPSE. They were obtained by the ratio of the two curves of the Fig. 5. It is immediately noticeable that for HIPSE, the detection efficiency as a function of the normalized E_{tr12} obtained for the studied events is very similar to that obtained as a function of the impact parameter B for these same events, knowing that E_{tr12} increases when the impact parameter B decreases (both curves in blue dotted line). This means that the efficiency of data experimental detection is better for central collisions, whereas it is less effective for peripheral collisions than for HIPSE (with the exception of the very peripheral collisions).

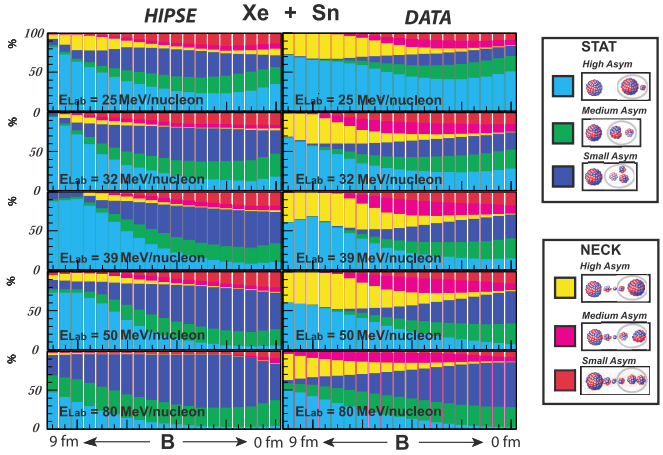

FIG. 6. Proportions of the various types of reaction mechanisms according to the experimental impact parameter (violence of the collision defined by normalized E_{tr12}) for collisions Xe + Sn at 25, 32, 39, 50, 80 MeV/nucleon.

We also want to study whether HIPSE can correctly reproduce the different reaction mechanisms (statistical events or events with neck emission), which have already been shown and discussed in Refs. [17,29,30], according to the deduced impact parameter and for collisions Xe + Sn at different incident energies. To determine the type of reaction mechanism, the same criterion as in Ref. [17] is used. We observe the presence (or not) of the second heaviest fragment of the forward part of the center of mass in the forward hemisphere of the QP frame (see Fig. 6). In this case it is a statistical event corresponding to a statistical emission by the hot nucleus. Otherwise it is a neck emission. But we must bear in mind that statistical emission is isotropic. Therefore we selected only half of the statistical contribution. The other one is necessarily emitted backwards and must therefore be removed from our selection of neck emission to obtain a selection corresponding to a pure neck emission. This is done specifically and only in Fig. 6.

At the same time, we studied another aspect: the asymmetry between the two heaviest fragments in the forward part of the center of mass. This is used to obtain the signal of bimodality associated with a liquid-gas phase transition in nuclei [31–33]. We should sign with this variable a possible transition between evaporation and multifragmentation when the quasiprojectile is deexcited. Figure 6 shows the relative proportions of these different mechanisms according to an experimental impact parameter. The discrepancy between the data and the HIPSE events can be seen: in particular HIPSE does not produce as much as neck emissions as experimental data. This could due to a high clusterization rate. The discrepancy appears to be particularly large for peripheral collisions. There is a slight improvement with the centrality of the collision for all the incident energies. It therefore seems necessary to improve the nuclear potential used. In this version of HIPSE the influence of angular momentum for the clusterization in terms of ℓ_{crit} has not been optimized. The discordance is most evident at 80 MeV/nucleon. The participant-spectator aspect becomes too important.

B. Study of the heaviest fragments at the front of the center of mass

Even if the proportions of events do not seem to be well reproduced, we will see that there is nevertheless a good match of physics for all different selections of events. We will first focus on studying the static and dynamic physical characteristics of the two heaviest fragments located at the front of the center of mass. We chose to study these physical quantities according to the violence of the collision using the transverse kinetic energy of LCPs. We have divided its experimental distribution into ten numbered bins of the same cross section, allowing for a selection of events according to the bin number associated with the event.

Figure 7 shows, on one hand, the average evolution of the charge of these two fragments according to the bin number of the normalized E_{tr12}, and on the other hand their average parallel velocities in the laboratory frame normalized to the initial projectile velocity, always according to the bin number of the normalized E_{tr12}. These two charges are important indicators of the process of deexcitation of the hot nuclei [31,34,35]. The heaviest fragment velocities supply an indication of the fraction of the initial incident energy, dissipated during the reaction. We focus on statistical collisions with a high asymmetry and collisions with a neck and a small asymmetry. In both cases, the agreement between the data and HIPSE is excellent for the reproduction of the average charge of both fragments.

A more global comparison, not presented here, realized for all the reaction mechanisms and for the incident energies 25, 32, 39, 50, and 80 MeV/nucleon, shows a relative discrepancy lower than 10% for the heaviest fragment and of the order of 15% for the second fragment. The agreement is slightly less good at 80 MeV/nucleon, where, at maximum, differences are of 15% and 20%. The event generator very reasonably reproduces the dispersion of the data around these mean values as we can see in Fig. 8. For all the incident energies, the relative difference between the data and HIPSE concerning the dispersion is lower, most of the time, than 20% for the maximum charge and between 20% and 25% for the second heaviest according to the asymmetry.

In Fig. 7 we also see that the experimental parallel mean velocity of the biggest fragment deviates from that simulated gradually as the collision becomes more violent. This effect is systematic for all the incident energies and reaction mechanisms. As part of our global comparison, it gives rise to a relative difference of 5%–15% depending on the violence of the collision for the highest asymmetry for all the mechanisms. There are few % to 10% remaining for the other asymmetries in the case of a neck emission and less than 5% in the case of statistical events. For the parallel velocity of second heaviest the trend is about the same for statistical events. For neck events there seems to be a small dependency on incident energy for small and medium asymmetries. For 50 and 80 MeV/nucleon, the difference is less or about 5%. For other incident energies it can reach 15% for medium asymmetry and 10% for small asymmetry.

Although HIPSE has shown limitations in reproducing the correct proportions for the various mechanisms, the

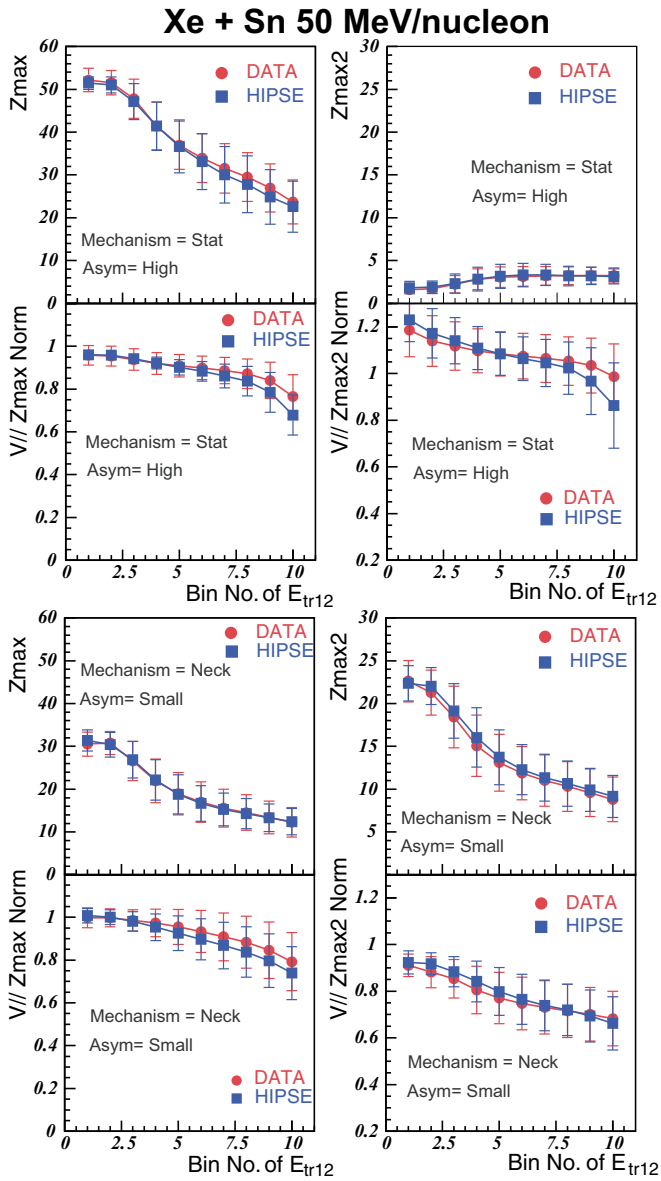

FIG. 7. Comparisons of mean charge and the mean parallel velocities of the two heaviest fragments at the front of the center of mass, between HIPSE and the data for various selections of collision violence. This study is made for two types of mechanism during collisions Xe + Sn at 50 MeV/nucleon.

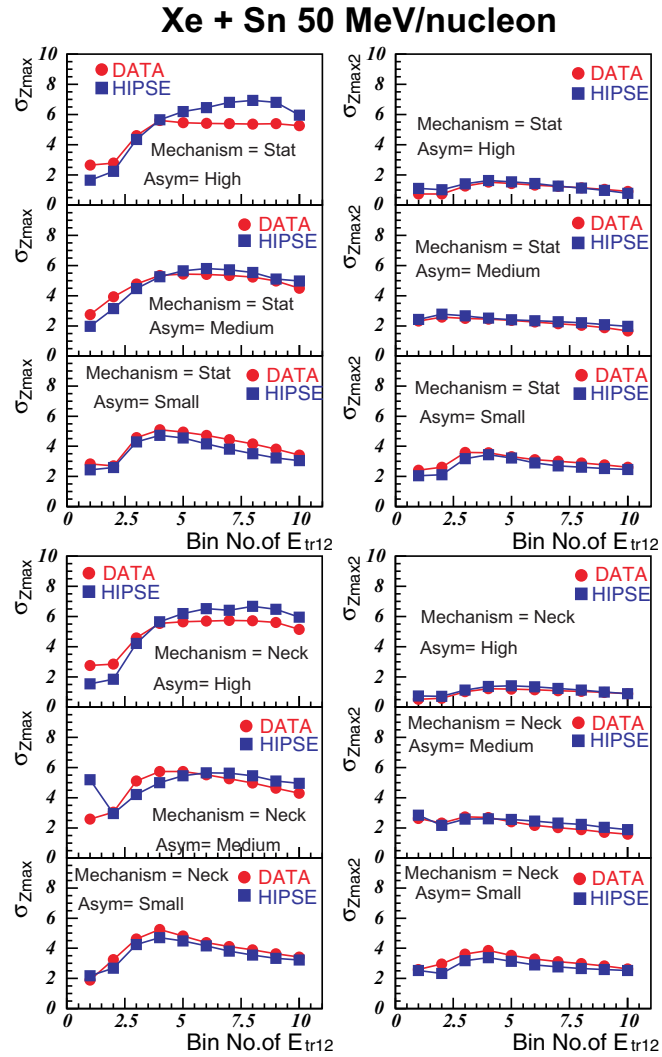

FIG. 8. Comparisons of the standard deviations of the distributions of charge of the two heaviest fragments in the front of the center of mass, obtained for HIPSE and the data for various selections of violence of collision. The first column corresponds to the Z_{max} and the second to the Z_{max2}. This study is made for both mechanisms and the three studied asymmetries during collisions Xe + Sn at 50 MeV/nucleon.

reasonable agreement is often greater than 10% concerning the physical characteristics of two heaviest fragments at the front of the center of mass and the study of the overall characteristics of the events made in Ref. [19] encourage us to continue basing our study on this simulation thereafter. We will then see that the physical characteristics of the QP reconstructed by the 3D calorimetry, for data and HIPSE, are very close. In addition, the quality of reproduction of the energetic and angular characteristics of certain LCPs in the QP frame provided by HIPSE [16,17] validates this choice even more.

III. STUDY OF THE 3D CALORIMETRY

A. Characterization of hot nuclei

We first chose to study only the system Xe + Sn at 50 MeV/nucleon. Figure 9(a) shows the evolution of QP excitation energy, and Fig. 9(b), the evolution of its charge as a function of the normalized E_{tr12}. To deduce these physical quantities, the 3D calorimetry was applied to the real data and HIPSE events filtered by INDRA. To verify the results obtained with 3D calorimetry, we performed a perfect calorimetry authorized by HIPSE that allows us to identify the particle origin in order to select only those emitted by the excited QP. This is why we applied this perfect calorimetry only with the ions actually detected by INDRA. Since, whatever experimental calorimetry used, it is impossible to

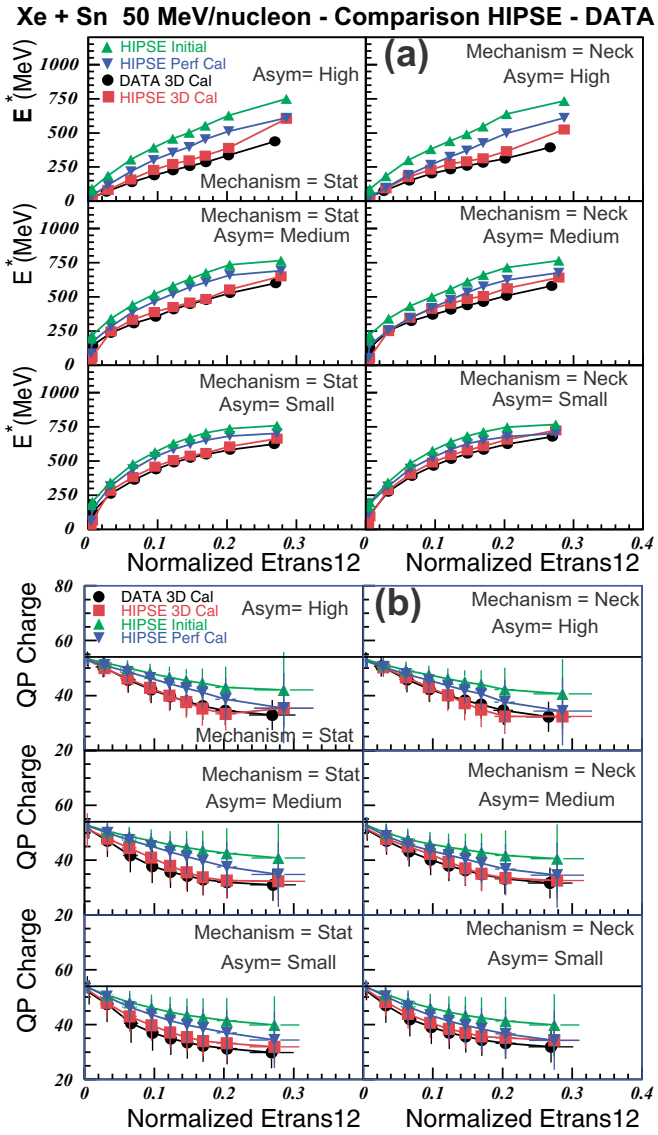

FIG. 9. (a) Mean correlations between the QP excitation energy and the normalized E_{tr12} found for data using 3D calorimetry and HIPSE using 3D calorimetry, perfect calorimetry and using true initial values. (b) Mean correlations between the QP charge and the normalized E_{tr12} found for the data by applying 3D calorimetry (full black circles) and for HIPSE by applying 3D calorimetry (full red squares), perfect calorimetry and using the true initial values supplied by the generator. This study is for the two types of mechanism and three asymmetries for Xe + Sn at 50 MeV/nucleon.

do a better calorimetry, we will take this perfect calorimetry as our reference. We added also the initial mean values of the physical quantities characterizing the QPs generated by HIPSE, which we wish to reproduce. All these results are presented for the different selections considered above.

The study of excitation energy clearly shows that we are not able to find the initial excitation energy of the QP, whatever the reaction mechanism and the system asymmetry, even with perfect calorimetry. The effect of the experimental device therefore seems problematic. The difference between the initial and reconstructed values tends to decrease with asymmetry. The reaction mechanism does not seem to play an obvious role. The values obtained with HIPSE seem to be at 50 MeV/nucleon always slightly higher than those obtained with data.

A more quantitative study of the QP excitation energy is therefore presented in Fig. 10; on one hand the relative difference observed between the data and HIPSE, for this physical quantity, when the 3D calorimetry is applied, and on the other hand the relative error on the measurement by comparing it with the true initial value, when it is made on the events generated by HIPSE (the calculations of these quantities are explained in Appendix). This complementary study is made for all the types of reaction mechanism and asymmetry, at 25, 32, 39, 50, and 80 MeV/nucleon. It is for the highest asymmetry that the difference between data and HIPSE is most important, especially for the highest incident energies. Most of time it remains below 20% except for the most violent collisions, where it begins to increase sharply to 40% and more depending on the incident energy. When asymmetry decreases, the agreement becomes much better, the difference becomes less than 10% and even close to 5% for the three lowest incident energies. There is a particular difference for very peripheral collisions linked partially to the poor detection of these collisions in the case of HIPSE but more particularly because of the right-left effect, shown and discussed in Refs. [16,17,23,36]. It is here more important in HIPSE than in the data because of the kinematics of the model. This tends to increase the apparent energy of the particles in the reconstructed frame. If we now look at Fig. 10(b), we find quantitatively that we are not able to determine the total excitation energy of the QP. With HIPSE, the relative error appears to be independent of the reaction mechanism. On the other hand, it evolves with asymmetry. We underestimate overall by 50%, 25%, and 15% when asymmetry decreases. For incident energies, 25 MeV/nucleon and 80 MeV/nucleon, the trends are even a little less good. This may be due to the INDRA filter being too strict for these incident energies, because it is a little less adapted to the characteristics of the data supplied by HIPSE, which are more forward focused than the data.

This complementary study therefore confirms, for all the incident energies, that the 3D calorimetry gives the same trends whatever the reaction mechanism. The agreement between HIPSE and the data and the quality of the measure of the excitation energy depends mainly on the asymmetry.

The study of the charge reconstruction in the Fig. 9(b) is also very interesting. Here again, regardless of the calorimetry used, perfect or 3D, we are not able to determine the initial mean charge of the QP. Perfect calorimetry seems to work a little better than for the excitation energy. The efficiency of detection always plays a major role. It is also necessary to note the very good agreement between the data and the simulation, when 3D calorimetry is applied.

Figure 11 confirms this quantitatively. The relative differences between data and HIPSE are independent of the reaction mechanism. They vary little with asymmetry. Overall, with the exception of the incident energy 80 MeV/nucleon, the difference is less than 10% and even 5% for semiperipheral

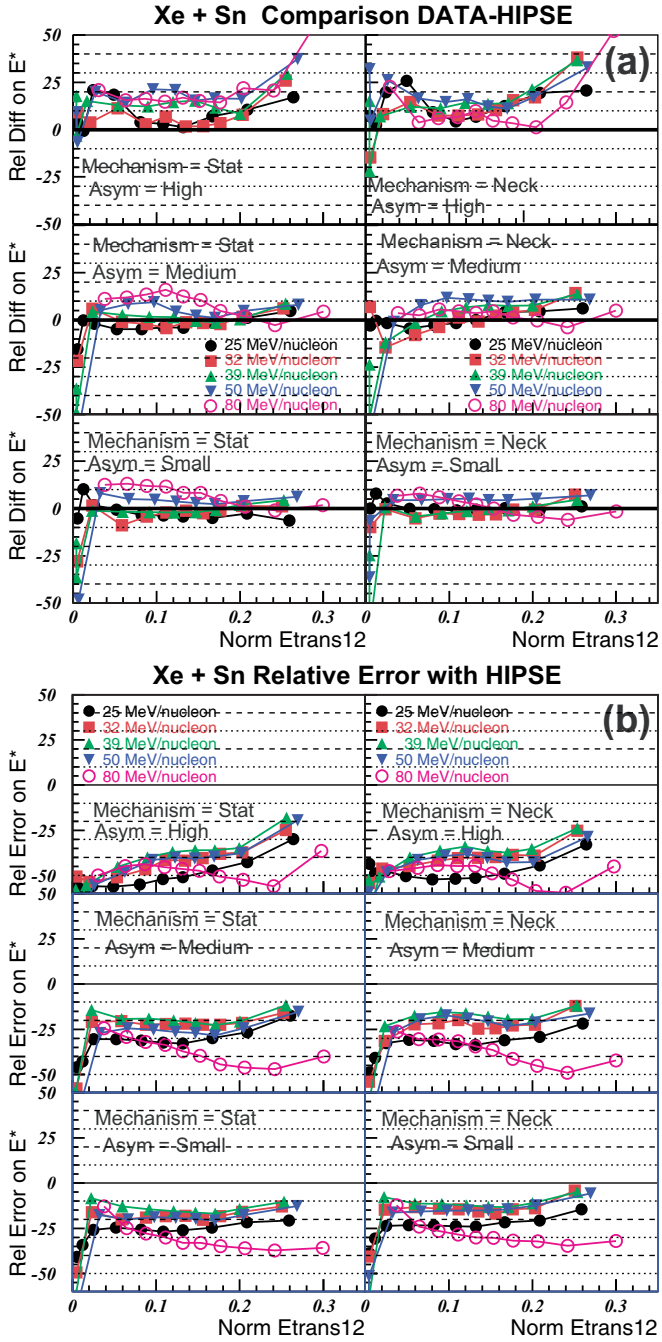

FIG. 10. (a) Study of the relative differences in % between the data and HIPSE obtained applying 3D calorimetry to measure the QP excitation energy, for all the studied selections. (b) Study of the relative errors in % on the measurement of the QP excitation energy when 3D calorimetry is applied to HIPSE, for all the studied selections. These studies are made for 25, 32, 39, 50, and 80 MeV/nucleon.

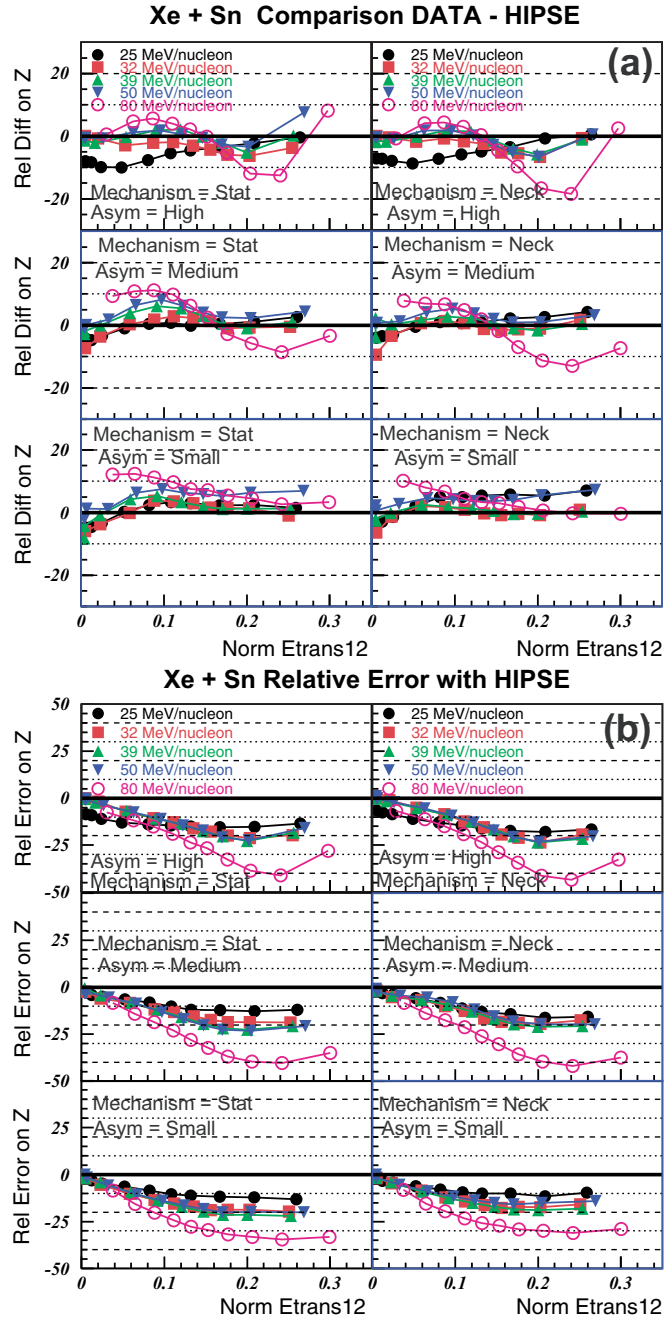

FIG. 11. (a) Study of the relative differences in % between the data and HIPSE obtained applying 3D calorimetry to measure the QP charge, for all the studied selections. (b) Study of the relative errors in % on the measurement of the QP charge when 3D calorimetry is applied to HIPSE, for all the studied selections. These studies are made for 25, 32, 39, 50, and 80 MeV/nucleon.

and central collisions whatever the incident energy. As a result, we note that as the reaction violence increases, more and more reaction products coming from QP emission are lost due to detector acceptance. The efficiency of detection decreases with the multiplicity until saturation. Figure 11(b) shows that the relative error of charge measurement is only null for the most peripheral collisions then it increases progressively up to about 25%. For peripheral collisions, the measurement error changes slightly with the incident energy. Then it becomes more important for 80 MeV/nucleon when centrality increases, then it reaches 30–40%. Figure 12(b) displays the QP mass for the usual selections. All the remarks concerning the QP charge also apply here to the QP mass,

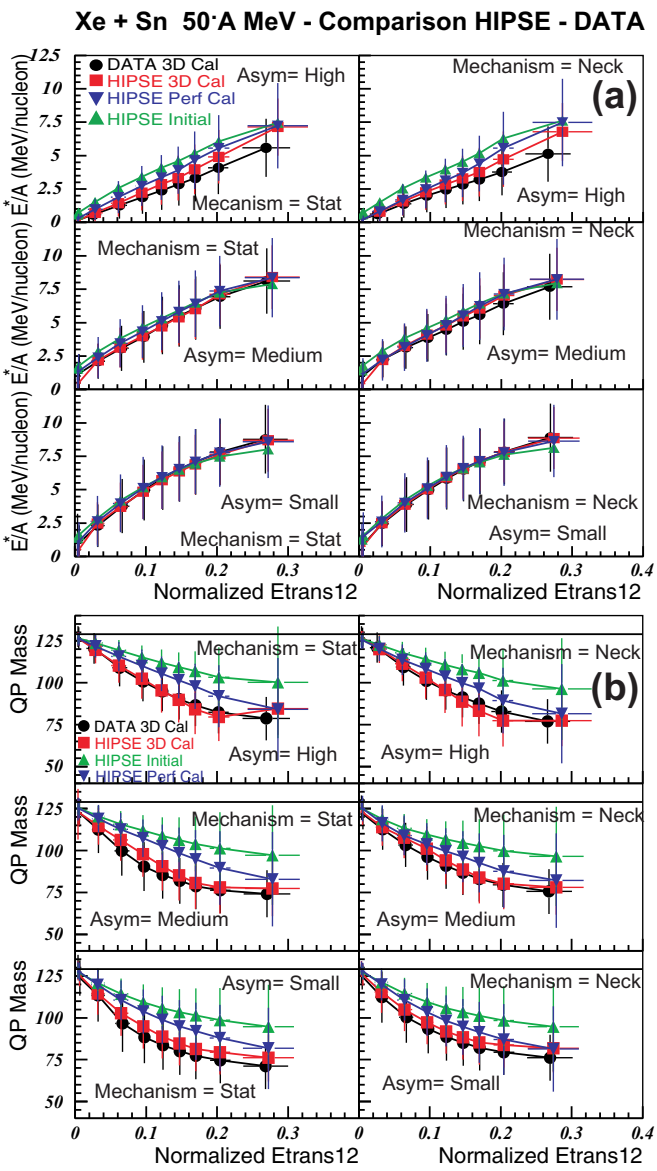

FIG. 12. (a) Mean correlations between the QP excitation energy per nucleon and the normalized E_{t12} found for the data applying 3D calorimetry and for HIPSE applying the 3D calorimetry, perfect calorimetry and using true initial values. (b) Mean correlations between the QP mass and the normalized E_{t12} found for the data applying 3D calorimetry (full black circles) and for HIPSE applying 3D calorimetry (full red squares), perfect calorimetry (full blue triangles), and using true initial values (full green triangles) supplied by the generator. This study is made for the two types of mechanism, three asymmetries during collisions Xe + Sn at 50 MeV/nucleon.

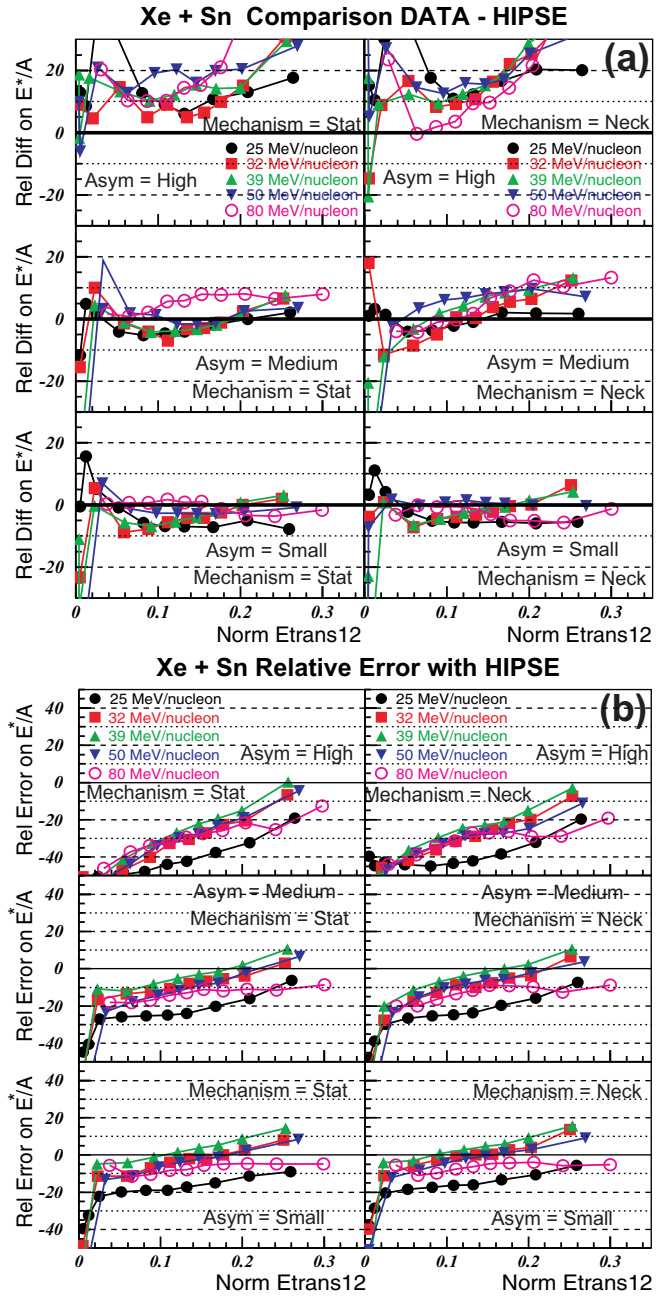

FIG. 13. (a) Study of the relative differences in % between the data and HIPSE obtained applying 3D calorimetry to measure the E^*/A of the QP, for all the studied selections. (b) Study of the relative errors in % on the measurement of the E^*/A of the QP when 3D calorimetry is applied to HIPSE, for all the studied selections. These studies are made for 25, 32, 39, 50, and 80 MeV/nucleon.

since it has been reconstructed from the initial isotopic ratio of the projectile.

In Fig. 12(a), for medium and small asymmetries, the agreement between data and HIPSE, concerning the measurements of the excitation energy per nucleon, appears quite remarkable considering the observations made previously on mass and excitation energy. It seems that, thanks to compensatory effects, the measurement of this last physical quantity seems better, especially for small asymmetries. In this case, 3D calorimetry applied to the data and HIPSE gives results similar to perfect calorimetry. They are all compatible with the initial value except for very peripheral and central collisions. The quantitative study, presented in Fig. 13, confirms this fact. There is a reasonable quality of measurement of excitation energy per nucleon for small asymmetries except for very peripheral and central collisions. For high asymmetries, there

is a systematic difference between data and HIPSE for both calorimetries. The excitation energy per nucleon is systematically greater in HIPSE than in the data by nearly 10%–20% for almost all incident energies, whatever the studied mechanism. This difference is greatly reduced with asymmetry; since for medium asymmetry, it becomes less than 10%. The data become moreover a little higher than HIPSE for the statistical collisions, contrary to those with neck. For small asymmetries, there are few differences between statistical collisions and collisions with neck, the data give values larger than HIPSE of 10%–0% depending on incident energy and centrality of the collision. On the other hand, we find again the very poor agreement already observed for very peripheral collisions corresponding to the first three zones of selection according to violence. Moreover the error on the measure of E^*/A follows slightly the same trends. The apparent quality of measurement depends on asymmetry, not on the mechanism of reaction. For high asymmetries, the excitation energy per nucleon is underestimated by 50% for the peripheral collisions. Then, the measure improves with the centrality of the reaction to reach between −10% and 0%. This trend is the same one for 32, 39, and 50 MeV/nucleon. For medium asymmetries, the mean relative errors evolve from −20%–10%, while for small asymmetries it is from −10%–15%. The measure for 25 MeV/nucleon is systematically less good of 10% approximately. For incident energy 80 MeV/nucleon, the trend appears also a little different, the error on the measure tends rather towards 0%.

From this analysis, we can therefore draw a certain number of conclusions:

(i) HIPSE very reasonably reflects the physics of collisions with small or medium asymmetries.

(ii) 3D Calorimetry gives results almost independent of the selected reaction mechanism (statistical or neck).

(iii) The measurement of the excitation energy per nucleon should be taken with caution (see Fig. 13). We have an accuracy of measurement on this physical quantity, which varies according to the asymmetry, the centrality and also to a lesser degree according to the studied system.

There is clearly a crucial influence of the detection device, which acts contradictorily according to the measured physical quantities. The charge and the mass are underestimated due to the efficiency of detection which seems normal. The measured excitation energy per nucleon can be higher than the original excitation energy per nucleon of the QP, which seems contradictory compared to the loss of a certain proportion of the particles evaporated by the QP. This implies an overestimation of the mean energy contribution of certain particles assigned by our method to the QP, which is also observable in the case of perfect calorimetry.

It also seems important to verify to what extent the calorimetry used increases the width of the distributions of excitation energy per nucleon. Excitation energy per nucleon is a fundamental quantity in nuclear thermodynamics and is often used to sort events and define event classes. We therefore present in Fig. 14(a) for the system Xe + Sn at 50 MeV/nucleon, the standard deviations observed for the various estimations of E^*/A of the QP and, in Fig. 14(b), we added the standard deviations on the mass of the rebuilt QP.

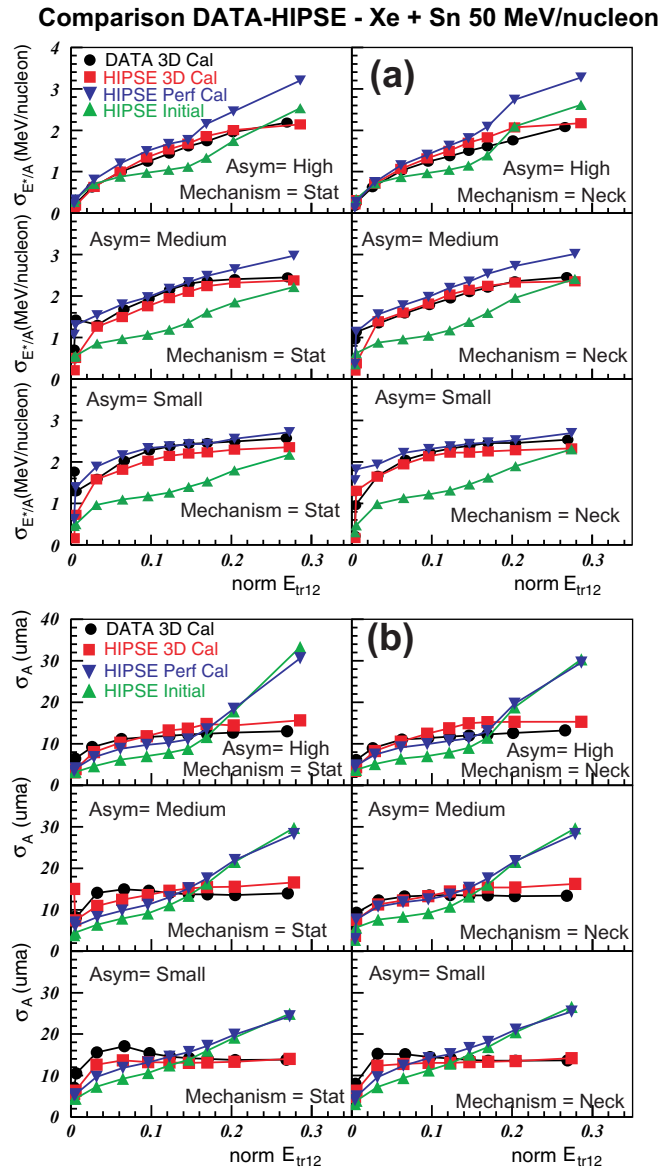

FIG. 14. (a) Mean correlations between the standard deviation on E^*/A of the QP and the normalized E_{tr12} found for the data applying 3D calorimetry and for HIPSE applying 3D calorimetry, perfect calorimetry and using true initial values. This study is made for both types of mechanism, three asymmetries during collisions Xe + Sn at 50 MeV/nucleon. (b) Mean correlations between the standard deviation on the QP mass and normalized E_{tr12} found for the data applying 3D calorimetry and for HIPSE applying 3D calorimetry, perfect calorimetry and using true initial values.

Concerning excitation energy per nucleon, the experimental fluctuations, obtained by 3D calorimetry with HIPSE, appear much larger than the initial fluctuations. They seem to increase with asymmetry without depending on the reaction mechanism, up to about twice as large for small asymmetries. They also do not follow the evolution of true initial fluctuations as a function of normalized transverse kinetic energy. There is a saturation of experimental measurements where the true initial values increase more clearly. The results obtained with

the data or HIPSE by applying 3D calorimetry are very close. These are only compatible with a perfect calorimetry for small asymmetries. The perfect calorimetry gives the largest fluctuations, again because of the influence of detection and especially the quality of the measurement of particle kinetic energy in the frame of the QP.

In Fig. 14(b), fluctuations on the measurement of QP mass give rise to different trends. For peripheral collisions, the experimental fluctuations obtained by applying 3D calorimetry are larger than the true fluctuations. Then, from a normalized transverse energy ranging between 0.15 and 0.17, the latter increase and become larger than the experimental fluctuations, which saturate. Only perfect calorimetry is capable of following the evolution of the true fluctuations while always being a little more important for peripheral and semiperipheral collisions. Again, the reaction mechanism does not seem to play a role. Experimental fluctuations are similar for data and HIPSE for high asymmetries. They vary for other asymmetries mainly for peripheral collisions. The data give slightly wider distributions.

The significant result in this figure is the impossibility for our calorimetry to determine the apparent widening of the QP mass distribution for central collisions. When we do a study similar at 25 MeV/nucleon, this trend is even more obvious. It seems to decrease as the incident energy increases. It should also be noted that it is more present and more important when asymmetry is important.

This result seems to show that our 3D calorimetry, based on probabilities defined from limited samples of evaporated particles, can only find the average behavior of the measured quantities and not the fluctuations. Another calorimetry can not do that either [36].

B. Study of the hot nucleus velocity

We already discussed in the previous sections the fundamental importance of the reference frame to characterize the energetic contribution of evaporation. We will now see to what extent it is possible to return to the kinematics of the QP formed during the reaction, by using our experimental 3D calorimetry. We continue to focus our attention again on the system Xe + Sn at 50 MeV/nucleon. We present in Fig. 15 the parallel and perpendicular components of different velocities, normalized to the velocity of the projectile in the laboratory. We are interested in the QP velocities rebuilt by 3D calorimetry, applied to data and to HIPSE. We also have two references: the initial QP velocity at the moment of the freeze-out in HIPSE and the velocity rebuild by perfect calorimetry, obtained with HIPSE.

The study of the parallel component shows that there is clearly, for all mechanisms and asymmetries, an obvious difference between the initial velocity at the freeze-out and the different reconstructed velocities. In fact, the opposite would have been abnormal. Indeed, it is necessary to take into account the Coulomb influence of the different partners of the collision during the deexcitation of the QP, which will be accelerated over time by the other participants. This influence is of course greater or lesser depending on the centrality of the collision, as can be seen in Fig. 15. Figure 16(b),

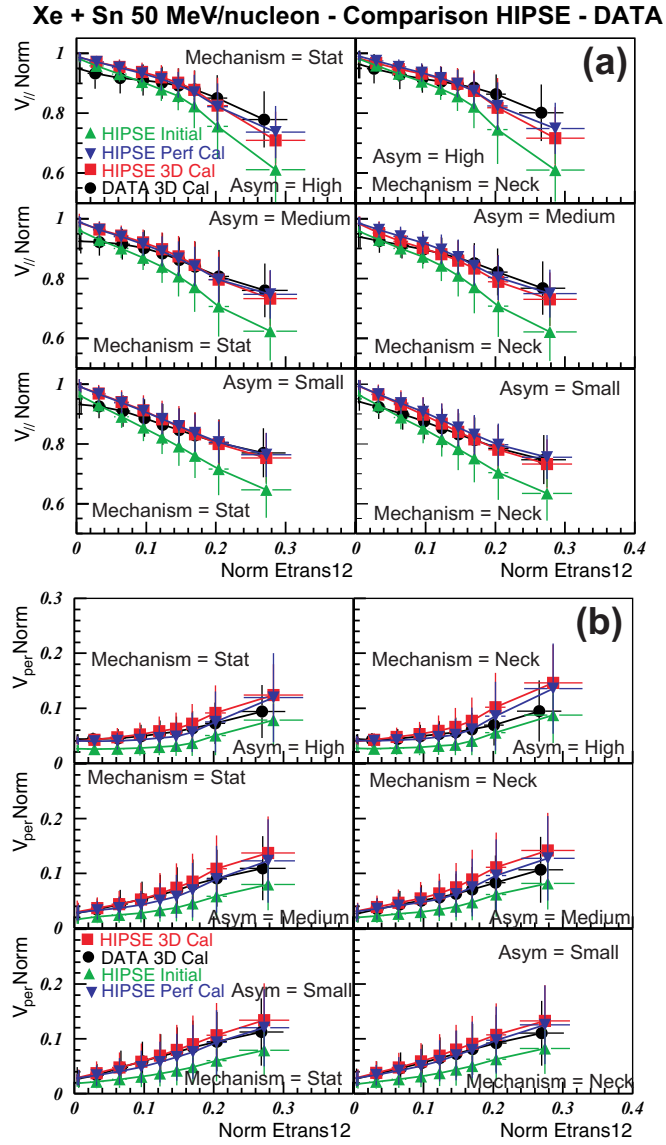

FIG. 15. (a) Mean correlations between the QP parallel velocity in the frame of the laboratory normalized to the velocity of the projectile and E_{tr12} normalized, found for the data applying 3D calorimetry and for HIPSE applying 3D calorimetry, perfect calorimetry and using true initial values. This study is made for the two types of mechanism, three asymmetries for collisions Xe + Sn at 50 MeV/nucleon. (b) Mean correlations between the QP perpendicular velocity in the frame of the laboratory normalized to the velocity of the projectile and E_{tr12} normalized, found for the data applying 3D calorimetry and for HIPSE applying 3D calorimetry, perfect calorimetry and using the true initial values.

which gives the relative measurement error on this quantity with HIPSE, completely confirms this fact for the relative comparison of the measured value and the initial value. The error is independent of the selected mechanism. It is lower for the highest incident energies and decreases with asymmetry, thus with the charge of the heaviest fragment. In experiments we will never have the opportunity to correct this effect, since we do not have the temporal sequence of emission of the

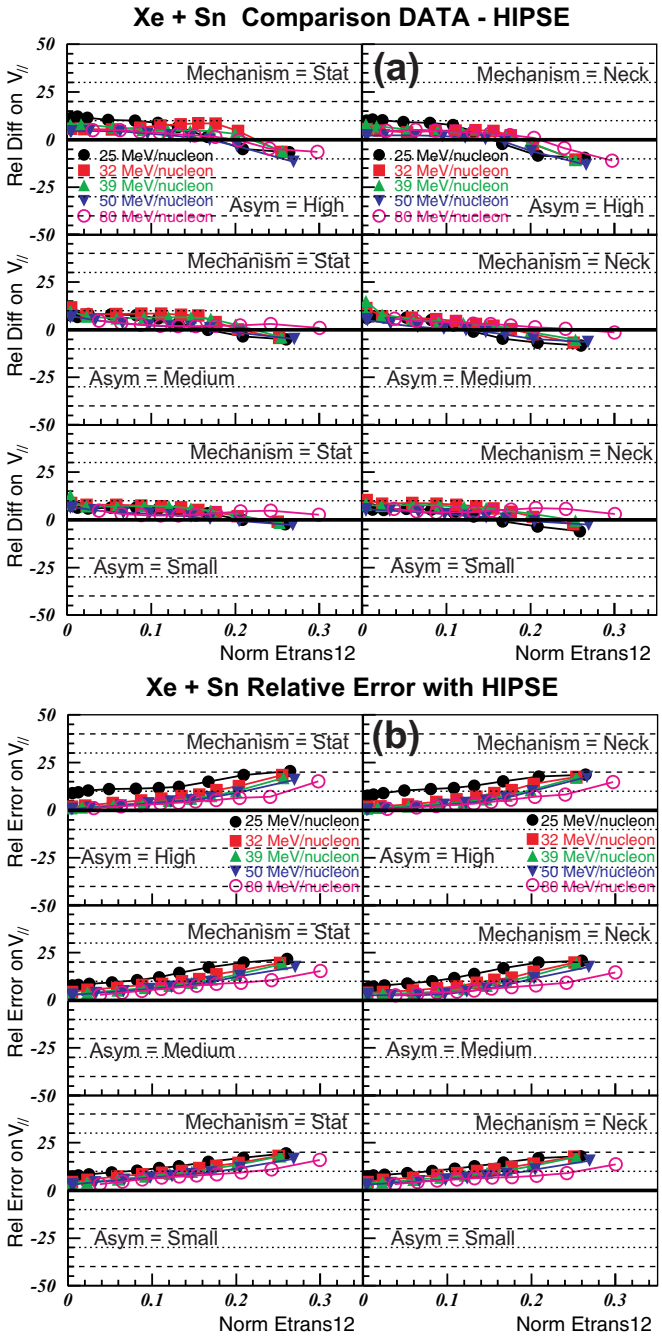

FIG. 16. (a) Study of the relative differences in % between the data and HIPSE obtained applying 3D calorimetry to measure the QP parallel velocity, for all the studied selections. (b) Study of the relative errors in % on the measurement of the QP parallel velocity when 3D calorimetry is applied to HIPSE, for all the studied selections. These studies are made for 25, 32, 39, 50, and 80 MeV/nucleon.

different particles. Figure 16, which also shows the difference between HIPSE and the data for the parallel component of the reconstructed QP, indicates that the relative variation is not important. It is in the order of 10% or less for peripheral collisions and tends towards 0 to −5% for central collisions. It depends very few on the reaction mechanism and varies little with incident energy except for 80 MeV/nucleon, which is always a special case and better. It is also important to note the remarkable agreement between 3D calorimetry and perfect calorimetry with respect to the reconstructed parallel component of the QP.

The data seem a little less compatible with HIPSE. It shows the small differences of kinematics already observed through transverse kinetic energy distributions and the difficulty of quantitatively reproducing the mechanisms of reaction.

Figure 15(b) allows an equivalent analysis of the component of the reconstructed velocity, perpendicular to the initial beam direction. We find an even greater difference between the initial and reconstructed values for all calorimetries. In this case, the Coulomb repulsion must also have an influence. The agreement between 3D calorimetry and perfect calorimetry is apparently less good than for the other component. There is also a larger difference between HIPSE and the data when 3D calorimetry is applied, mainly for the most violent collisions.

The dynamics of the collision must be partially responsible, as shown in Fig. 17 where the quality of the measurement of the QP polar angle in the laboratory frame is displayed. First, we observe a clear apparent difference in kinematics between HIPSE and the data whatever the mechanism or asymmetries. We also note a significant relative error on the experimental determination of this angle, between 50% and 150% in all situations. The Coulomb repulsion between the collision partners must play some role in this trend. These two polar angles are not determined at the same time of the collision. The initial polar angle is defined at the moment of freeze-out, while the measured angle is determined at the moment of detection of the reaction products, long after the two partners have separated. The action of the Coulomb repulsion can be important during this interval of time.

Figure 17(a) shows the relative difference between the data and HIPSE on the mean angle $\theta_{\rm lab}$, the angle between the reconstructed velocity and the initial beam direction in the laboratory frame. It can be noted that a correct match between HIPSE and the data seems to exist only for peripheral collisions at 50 and 80 MeV/nucleon. It is for these that the role of the reaggregation is minimal in HIPSE. The correct treatment of the interaction between the nuclei at small angles must reflect the shape of the edges of the nuclei and must be treated by quantum mechanics. It is interesting to note that in peripheral collisions, the angular distributions of the QP for 25, 32, and 39 MeV/nucleon are more focused forward for HIPSE than for the data.

In Fig. 17(b) we present the error on the measurement of this angle in the HIPSE model, always for the same incident energies. It can be seen that the quality of the measurement depends little on the mechanism and asymmetry but much more on the incident energy. Whatever the latter, the measure seems bad. The relative error fluctuates between 50 and 150%. The initial polar angle at the freeze-out should be also different from that measured long after because of the influence of Coulomb repulsion.

This average angle is very sensitive to the experimental device used. The angular resolution limited by INDRA implies a distortion of the angular distribution of particles detected in the frame of the laboratory. We are indeed obliged to randomize the direction of the velocity of each detected

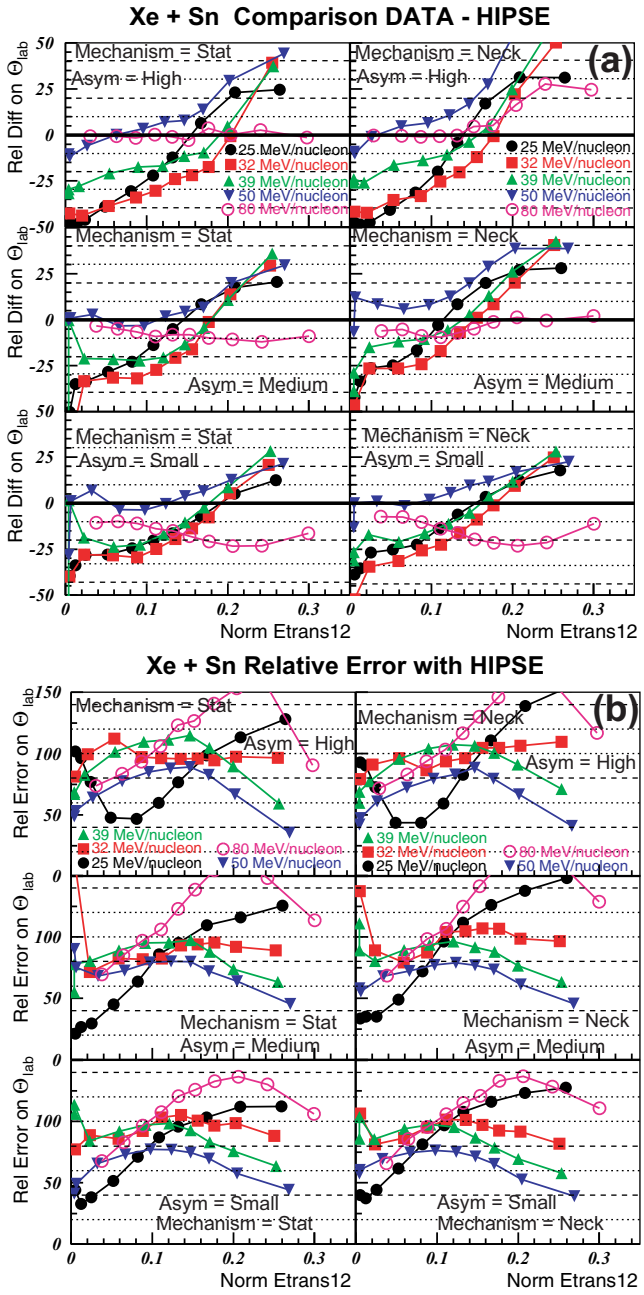

FIG. 17. (a) Study of the relative differences in % between the data and HIPSE obtained applying 3D calorimetry to measure the QP polar angle in the laboratory frame, for all the studied selections. (b) Study of the relative errors in % on the measurement of the QP polar angle in the laboratory frame when 3D calorimetry is applied to HIPSE, for all the studied selections. These studies are made for 25, 32, 39, 50, and 80 MeV/nucleon.

particle over the entire solid angle under which the detection module is seen from the target. This is not done by taking into account the real spatial distribution of particles, because it is not known. Another reason, which could explain this result, is the influence of the beam hole. This prevents the detection of particles at small angles, favoring a larger average angle of the reconstructed QP. Small imperfections, which may exist in the software filter, can also contribute to the differences between reality and simulation. Finally, we must remember that these angles have mainly a small value, therefore even a small absolute error gives a large relative error.

IV. CONCLUSIONS

In a previous paper [17], a new calorimetry of the quasiprojectile, aiming to be optimal, was proposed. It tries to take into account in the best possible way the different contributions that can exist in a heavy-ion collision at Fermi energies. This calorimetry is based on the experimental determination of an evaporation probability from the physical characteristics of the particles in a restricted velocity space domain.

HIPSE is an event generator trying to integrate all phenomena that can occur at Fermi energies. It is convenient and fast. It seemed interesting to use this generator to study and validate this new calorimetry called 3D calorimetry. The application of this experimental calorimetry to the real data and events generated by HIPSE allowed us to have some control of measurements by constantly comparing them.

The first important result of this study was the demonstration of the enormous influence of the experimental device but not as one might expect. The need for the most complete event detection for correct calorimetry generates an extremely spurious effect for some collisions, especially those with a heavy forward-focused evaporation residue, so often with a high asymmetry between the two heaviest fragments at the front of the center of mass. In fact, the completeness criteria require selecting events with a very particular topology in the velocity space. In fact, in these events, to be detected, the QP residue must necessarily avoid passing through the beam hole made to let the beam pass. The linear momentum conservation requires a LCP contribution sufficiently energetic to permit that. It is the effect known as right-left effect, already observed [16,17,23,36], which is largely responsible for the apparent degradation of the experimental QP characterization. In the QP frame, it contributes to an overestimation of the average energy contribution of some particle allocated by calorimetry to the QP. This overestimation is also observed in the case of perfect calorimetry. The nonevaporative contribution, the experimental measurement of the kinetic energy of each particle by INDRA, and the determination of the emitter velocity are others sources of errors for 3D calorimetry. These last causes must also be responsible for errors observed for a perfect calorimetry.

The second important result is that the 3D calorimetry is equivalent to perfect calorimetry when the influence of the right-left effect is minimal. The correction of this effect is complex because it is intimately linked to the collision dynamics, therefore depends on the impact parameter, the incident energy and the studied system. HIPSE reasonably reproduces the data for small and medium asymmetries, less for high asymmetries. This is also partly explained by this effect, since the collision dynamics are not perfectly reproduced mainly for peripheral collisions.

The fact that the reconstructed velocity obtained by the 3D calorimetry and the perfect calorimetry are close whatever the mechanism and the asymmetry, with the exception of the last

two selections of violence, makes us think that the angular resolution of the detector also plays a fundamental role in these difficulties of measurement of the excitation energy. We must also bear in mind that for HIPSE, we compare the kinematics at the freeze-out moment and a reconstructed kinematics at the end of the cooling. The Coulomb repulsion must also disrupt these measures.

We have not studied the role that the estimation of the neutral contribution can have on the determination of excitation energy. It has yet to be accomplished. It should also be noted that this 3D calorimetry, like other calorimetries, does not allow an accurate estimation of the width of distributions of the physical quantities characteristic of the QP. This disturbs us to make correct unmixed microcanonical selections of the events.

For good calorimetry, it is necessary to clearly improve the geometric efficiency, especially at the front, granularity, angular resolution, and mass resolution of the experimental device. It is a very difficult challenge knowing the experimental qualities of INDRA.

We have also demonstrated that validation of the new experimental calorimetry, using an event generator and a filter of the experimental setup, is mandatory. This should also allow us to define the parameters of correction for the real data if we want to improve our 3D calorimetry to take into account the defects of the experimental device. But the quality of this correction depends on the realism of these two elements.

APPENDIX: PRINCIPLES OF CALCULATIONS OF THE DIFFERENCE AND OF THE ERROR

To calculate the relative difference on a physical quantity X measured by the experimental calorimetry between the data and HIPSE, we use the following relation:

$$\text{Rel Difference on } X = 100\% \times \frac{X_{\text{HIPSE}} - X_{\text{DATA}}}{X_{\text{DATA}}}. \quad \text{(A1)}$$

To calculate the relative error on a physical quantity X between the result of the measure by the experimental calorimetry and the real initial value X_{INI}, for the events supplied by HIPSE and filtered, we use the following relation:

$$\text{Rel Error on } X = 100\% \times \frac{X_{\text{HIPSE}} - X_{\text{INI}}}{X_{\text{INI}}}. \quad \text{(A2)}$$

[1] G. Lehaut, D. Durand, O. Lopez, E. Vient, A. Chbihi, J. D. Frankland, E. Bonnet, B. Borderie, R. Bougault, E. Galichet, D. Guinet, P. Lautesse, N. Le Neindre, P. Napolitani, M. Parlog, M. F. Rivet, and E. Rosato, Phys. Rev. Lett. **104**, 232701 (2010).

[2] O. Lopez, D. Durand, G. Lehaut, B. Borderie, J. D. Frankland, M. F. Rivet, R. Bougault, A. Chbihi, E. Galichet, D. Guinet, M. LaCommara, N. Le Neindre, I. Lombardo, L. Manduci, P. Marini, P. Napolitani, M. Pârlog, E. Rosato, G. Spadaccini, E. Vient, and M. Vigilante, Phys. Rev. C **90**, 064602 (2014).

[3] H. Fuchs and K. Mohring, Rep. Prog. Phys. **57**, 231 (1994).

[4] J. C. Steckmeyer, A. Kerambrun, J. C. Angélique, G. Auger, G. Bizard, R. Brou, C. Cabot, E. Crema, D. Cussol, D. Durand, Y. El Masri, P. Eudes, M. Gonin, K. Hagel, Z. Y. He, S. C. Jeong, C. Lebrun, J. P. Patry, A. Péghaire, J. Péter, R. Régimbart, E. Rosato, F. Saint-Laurent, B. Tamain, E. Vient, and R. Wada, Phys. Rev. Lett. **76**, 4895 (1996).

[5] B. Lott, S. P. Baldwin, B. M. Szabo, B. M. Quednau, W. U. Schröder, J. Tõke, L. G. Sobotka, J. Barreto, R. J. Charity, L. Gallamore, D. G. Sarantites, D. W. Stracener, and R. T. de Souza, Phys. Rev. Lett. **68**, 3141 (1992).

[6] S. P. Baldwin, B. Lott, B. M. Szabo, B. M. Quednau, W. U. Schröder, J. Tõke, L. G. Sobotka, J. Barreto, R. J. Charity, L. Gallamore, D. G. Sarantites, D. W. Stracener, and R. T. de Souza, Phys. Rev. Lett. **74**, 1299 (1995).

[7] R. Bougault *et al.*, Nucl. Phys. A **587**, 499 (1995).

[8] L. Stuttgé *et al.*, Nucl. Phys. A **539**, 511 (1992).

[9] J. Töke *et al.*, Nucl. Phys. A **583**, 519 (1995).

[10] J. Łukasik *et al.*, Phys. Rev. C **55**, 1906 (1997).

[11] F. Bocage *et al.*, Nucl. Phys. A **676**, 391 (2000).

[12] M. Di Toro, A. Olmi, and R. Roy, Eur. Phys. J. A **30**, 65 (2006).

[13] M. Germain *et al.*, Phys. Lett. B **488**, 211 (2000).

[14] T. Lefort *et al.*, Nucl. Phys. A **662**, 397 (2000).

[15] V. Viola and R. Bougault, Eur. Phys. J. A **30**, 215 (2006).

[16] E. Vient, Habilitation à diriger des recherches, Université de Caen,2006, URL https://tel.archives-ouvertes.fr/tel-00141924.

[17] E. Vient *et al.*, Phys. Rev. C **98**, 044611 (2018).

[18] J. Pouthas *et al.*, Nucl, Instr. Meth. Phys. A **357**, 418 (1995).

[19] D. Lacroix, A. Van Lauwe, and D. Durand, Phys. Rev. C **69**, 054604 (2004).

[20] N. Copinet, Ph.D. thesis, Université de Caen, 1990.

[21] D. Cussol, E. Plagnol, and O. Tirel (private communication).

[22] D. Lacroix, V. Blideanu, and D. Durand, Phys. Rev. C **71**, 024601 (2005).

[23] J. C. Steckmeyer *et al.*, Nucl. Phys. A **686**, 537 (2001).

[24] N. Marie, Ph.D. thesis, Université de Caen, 1995.

[25] J. Péter *et al.*, Phys. Lett. B **237**, 187 (1990).

[26] C. Cavata, M. Demoulins, J. Gosset, M.-C. Lemaire, D. L'Hôte, J. Poitou, and O. Valette, Phys. Rev. C **42**, 1760 (1990).

[27] D. R. Bowman, C. M. Mader, G. F. Peaslee, W. Bauer, N. Carlin, R. T. de Souza, C. K. Gelbke, W. G. Gong, Y. D. Kim, M. A. Lisa, W. G . Lynch, L. Phair, M. B. Tsang, C. Williams, N. Colonna, K. Hanold, M. A. McMahan, G. J. Wozniak, L. G. Moretto, and W. A. Friedman, Phys. Rev. C **46**, 1834 (1992).

[28] L. Phair *et al.*, Nucl. Phys. A **548**, 489 (1992).

[29] J. Colin, D. Cussol, J. Normand, N. Bellaize, R. Bougault, A. M. Buta, D. Durand, O. Lopez, L. Manduci, J. Marie, J. C. Steckmeyer, B. Tamain, A. Van Lauwe, E. Vient, B. Borderie, F. Lavaud, N. Le Neindre, P. Pawłowski, E. Plagnol, M. F. Rivet, B. Bouriquet, A. Chbihi, J. D. Frankland, D. Guinet, B. Guiot, S. Hudan, J. P. Wieleczko, J. L. Charvet, R. Dayras, E. Galichet, P. Lautesse, L. Nalpas, M. Pârlog, E. Rosato, R. Roy, M. Vigilante, and C. Volant, Phys. Rev. C **67**, 064603 (2003).

[30] J. Normand, Ph.D. thesis, Université de Caen, 2001.

[31] M. Pichon *et al.*, Nucl. Phys. A **779**, 267 (2006).

[32] E. Bonnet, D. Mercier, B. Borderie, F. Gulminelli, M. F. Rivet, B. Tamain, R. Bougault, A. Chbihi, R. Dayras, J. D. Frankland, E. Galichet, F. Gagnon-Moisan, D. Guinet, P. Lautesse, J. Łukasik, N. Le Neindre, M. Pârlog, E. Rosato, R. Roy, M. Vigilante, J. P. Wieleczko, and B. Zwieglinski, Phys. Rev. Lett. **103**, 072701 (2009).

[33] M. Bruno, F. Gulminelli, F. Cannata, M. D'Agostino, F. Gramegna, and G. Vannini, Nucl. Phys. A **807**, 48 (2008).

[34] B. Borderie, G. Tăbăcaru, P. Chomaz, M. Colonna, A. Guarnera, M. Pârlog, M. F. Rivet, G. Auger, C. O. Bacri, N. Bellaize, R. Bougault, B. Bouriquet, R. Brou, P. Buchet, A. Chbihi, J. Colin, A. Demeyer, E. Galichet, E. Gerlic, D. Guinet, S. Hudan, P. Lautesse, F. Lavaud, J. L. Laville, J. F. Lecolley, C. Leduc, R. Legrain, N. Le Neindre, O. Lopez, M. Louvel, A. M. Maskay, J. Normand, P. Pawłowski, E. Rosato, F. Saint-Laurent, J. C. Steckmeyer, B. Tamain, L. Tassan-Got, E. Vient, and J. P. Wieleczko, Phys. Rev. Lett. **86**, 3252 (2001).

[35] J. D. Frankland, A. Chbihi, A. Mignon, M. L. Begemann-Blaich, R. Bittiger, B. Borderie, R. Bougault, J.-L. Charvet, D. Cussol, R. Dayras, D. Durand, C. Escano-Rodriguez, E. Galichet, D. Guinet, P. Lautesse, A. Le Févre, R. Legrain, N. Le Neindre, O. Lopez, J. Łukasik, U. Lynen, L. Manduci, J. Marie, W. F. J. Müller, L. Nalpas, H. Orth, M. Pârlog, M. Pichon, M. F. Rivet, E. Rosato, R. Roy, A. Saija, C. Schwarz, C. Sfienti, B. Tamain, W. Trautmann, A. Trczinski, K. Turzó, A. Van Lauwe, E. Vient, M. Vigilante, C. Volant, J. P. Wieleczko, and B. Zwieglinski, Phys. Rev. C **71**, 034607 (2005).

[36] E. Vient *et al.*, Nucl. Phys. A **700**, 555 (2002).